



Auristatin F-Delivering SNAP-Tag Based Recombinant Antibody-Drug Conjugate Targeting *EpCAM* Demonstrating Selective In vitro Killing of Cervical and Triple-Negative Breast Cancer Cell Lines

Ursula-Claire Andong-Koung-Edzidzi¹, Thabo Matshoba¹, Dirk Lang², Roger Hunter³ and Stefan Barth^{*1,4}

Abstract

Background: Triple-negative breast cancer is an aggressive subtype of breast cancer lacking the ER, PR, and HER2 receptor. Hence, standard treatment is limited. Cervical cancer is considered a preventable cancer since it often occurs secondary to long-term high-risk HPV infection. Vaccines against the virus are available and globally have resulted in reduced incidence and mortality yet, in some regions cervical cancer remains the second cause of cancer related mortality in women, second only to breast cancer. Therefore, the importance of a single effective and specific treatment against both cancers could not be understated.

Methodology: scFv-SNAP-tag based fusion protein was transiently expressed in a mammalian expression system, and the secreted proteins were isolated from cell culture supernatants by immobilized metal affinity chromatography. Subsequently, auristatin F (AURIF) anticancer drug was conjugated to the scFv-SNAP to assess the dose-dependent activity of the therapeutic protein on EpCAM-positive TNBC and cervical cancer cell lines.

Results: The surface binding of the fluorescently labelled SNAP-tag based fusion protein was observed across all cell lines; however, internalization was seen on one EpCAM-positive TNBC and all cervical cancer cell lines. The α EpCAM(scFv)-SNAP-linker-AURIF (ADC) demonstrated dose-dependent killing on target cell lines.

Conclusion: Fluorophore labelled α EpCAM(scFv)-SNAP works well in flow cytometry and fluorescent microscopy, and can be further exploited as a diagnostic tool. The ADC demonstrated selective killing of highly EpCAM-positive cell lines. This might have further implications for future human application as a prescreening of patients might allow to identify the ones with higher expression levels benefitting from such an EpCAM targeting immunotherapy.

Keywords: Triple-negative breast and cervical cancer, recombinant antibody-drug-conjugate, diagnostic, therapeutic, Epithelial cell adhesion molecule (EpCAM), SNAP-tag.

Background

Antibody drug conjugates (ADCs) have been established as one of the most promising class of anti-tumour agents that can deliver cytotoxic drugs attached to monoclonal antibodies via specific conjugation. They were designed to improve the efficacy and reduce the toxicity of highly potent

Affiliation:

¹Medical Biotechnology and Immunotherapy Research Unit, Department of Integrative Biomedical Sciences, Institute of Infectious Disease and Molecular Medicine, Faculty of Health Sciences, University of Cape Town, Cape Town 7700, South Africa.

²Division of Physiological Sciences, Department of Human Biology, University of Cape Town, Cape Town 7700, South Africa.

³Department of Chemistry, PD Hahn Building, University of Cape Town, Cape Town 7700, South Africa.

⁴South African Research Chair in Cancer Biotechnology, Department of Integrative Biomedical Sciences, Faculty of Health Sciences, University of Cape Town, Cape Town 7700, South Africa

*Corresponding author:

Stefan Barth. Medical Biotechnology and Immunotherapy Research Unit, Department of Integrative Biomedical Sciences, Institute of Infectious Disease and Molecular Medicine, Faculty of Health Sciences, University of Cape Town, Cape Town 7700, South Africa.

Citation: Ursula-Claire Andong-Koung-Edzidzi, Thabo Matshoba, Dirk Lang, Roger Hunter and Stefan Barth. Auristatin F-Delivering SNAP-Tag Based Recombinant Antibody-Drug Conjugate Targeting *EpCAM* Demonstrating Selective In vitro Killing of Cervical and Triple-Negative Breast Cancer Cell Lines. Journal of Pharmacy and Pharmacology Research. 10 (2026): 1-14.

Received: December 08, 2025

Accepted: December 15, 2025

Published: January 06, 2026

drugs which are too toxic to be systematically administered on their own. They eliminate cancer cells by binding to cell surface receptors differentially overexpressed on a tumor cell before being internalized and routed to lysosomes where the protein is degraded by proteases and the active synthetic payload released into the cytosol to interact with various cellular mechanisms to induce cell death [1-2]. The most common active payloads for ADCs formulation are tubulin-inhibiting agents. These agents are preferentially accumulated in highly proliferating cells that enables some discrimination between tumour and normal cells [3]. Marine toxins isolated from marine organisms have been shown to have anticancer properties. Among the marine cytotoxins, dolastatin 10 is a highly potent antimitotic compound isolated from the sea hare *Dolabella auricularia*. Because of off-target toxicities, dolastatin 10 failed in clinical trials as a single anti-cancer agent and was replaced by its derivatives: Monomethyl Auristatin E (MMAE) and Monomethyl Auristatin F (MMAF) which are current examples of payloads used in ADC formulations. [4]. The mechanism of action of MMAE (AURIE) and MMAF (AURIF) involves the inhibition of tubulin polymerization, thus blocking tubulin assembly, which consequently activates G2/M cell cycle phase arrest causing cells to undergo apoptosis. Brentuximab Vedotin is an anti-CD30 monoclonal antibody conjugated to AURIE and was approved by the FDA in 2011 for the treatment of relapsed Hodgkin Lymphoma after stem cell transplantation. However, AURIE was shown to cause more adverse side effects as a free drug compared to AURIF due to their physicochemical difference affecting membrane permeability [5]. The internalization of corresponding ADCs by target cells resulted in the cleavage of the linker and lysosomal degradation releasing free AURIE, consequently causing a bystander effect. This effect can either be advantageous because it will cause the death of the antigen-positive targeted cells or disadvantageous because the antigen-negative cells will also die. Conversely, antibody conjugated to AURIF via a non-cleavable linker releases potent AURIF bound to the cysteine residue, thus lacking bystander effect due to the strongly reduced ability of the drug to permeate via cell membranes because of its charged C-terminal phenylalanine residue. These types of ADCs are (1) highly stable, (2) demonstrating effective anti-tumor activity after internalization and lysosomal degradation, and (3) show highest anti-cancer efficacy with high and homogeneous expression of target antigens on tumor cells [6].

The selection of suitable antigens is crucial for the generation of ADCs, independent of their overexpressions which are needed for internalization upon binding [7]. Epidermal cell adhesion molecule (EpCAM) is one of the earliest tumour associated antigens identified. The gene expressing EpCAM is located on chromosome 2, band 2p21 and the gene product shares 50% homology with GA733-

1 also called Trop-2 (located on chromosome 1), hence EpCAM is sometimes referred to as GA733-2 (Trop-1), or CD326 [8-9]. EpCAM is a 40 kDa type I transmembrane glycoprotein composed of 314 amino acids, which mediates cell-cell adhesion. The structure of EpCAM consists of an extracellular domain (EpEX) divided into 3 domains, a single transmembrane domain and an intracellular domain (EpICD). Immunotherapeutics targeting EpCAM such as Edrecolomab, Adecatumumab and Catumaxomab typically bind to 17-1A, GA733 or AUA-1 all of which are located on domain I of the extracellular portion of the protein. The thyroglobulin-like portion on domain II of the extracellular domain is necessary for the mediation of cell-cell adhesion. Its cytoplasmic domain, in addition to being involved in signal transduction leading to regulation of gene expression, is also contributing to cell adhesion through interactions with the cellular cytoskeleton. As a cell-to-cell contact molecule, EpCAM can also transmit signals from the cell membrane all the way to the nucleus. In embryonic stem cells, EpCAM is highly expressed and is necessary for maintenance of the self-renewal properties and pluripotency of the cells [10]. Signalling is initiated by intramembrane proteolysis through the action of tumour necrosis factor α converting enzyme (TACE), followed by proteolytic cleavage by γ -secretase complexes which leaves only the soluble intracellular portion of EpCAM (EpICD). EpICD forms a complex with FHL2 and β -catenin, and translocates to the nucleus where gene expression is regulated. *C-myc* is one of the genes whose expression is affected by EpCAM signalling, and has been linked with the induction of stem-like transcription profile in cancer cells[11-12]. N-glycosylation of an asparagine on the most membrane proximal glycosylation site seems to give a 3-fold increase in the half-life of membrane bound EpCAM in tumour cells. Following from this, EpCAM was found to be hyperglycosylated in a majority of carcinomas compared to healthy tissue analogues. This may explain its overexpression in primary and metastatic tumours compared to normal tissues and its association with CSCs. Hence, due to the high expression of EpCAM in adenocarcinomas and squamous cell carcinomas of various origins and the previously described efficacy of EpCAM targeting immunotherapies[13], we generated an AURIF SNAP-tag based ADC targeting EpCAM antigen positive cells. The selective targeting of TNBC and cervical cancer at nanomolar range using the SNAP-tag technology demonstrated the delivery of AURIF as a novel strategy against both types of cancer.

Results

Expression and production of the SNAP-tag based recombinant fusion protein

Upon in-silico design (figure 1a), the potential recombinant plasmid DNA was isolated using various molecular biology techniques prior to sequencing to confirm

successful ligation/insertion of α EpCAM(scFv) insert to the pCB-SNAP backbone. SnapGene software was used to confirm the integrity of the cloned product by aligning the chromatogram generated by sanger sequencing with the original in-silico sequence encoding the 10x His-tag. The pCB- α EpCAM(scFv)-SNAP clone showed approximately 100% homology with the in-silico ORF sequence, thus confirming successful sequencing.

The recombinant fusion protein was transiently transfected into HEK293T cells for protein expression. The transfected cells were monitored by fluorescent imaging for eGFP expression as an indicator for cells expressing the construct DNA (figure 1b). Thereafter, flow cytometry was done to quantify eGFP expression in each population as an indication of cells positive for the pCB expression vector and thus likely to express and secrete the desired proteins. The brightfield image showed that many cells were present in a specific area while the greenfield image indicated that most of these cells were positive for eGFP. The percentage of cells expressing the putative fusion protein was 72.7 % (figure 1c). It is worth mentioning that the high transfection efficiency was achieved by increasing the incubation time of the complex mixture (transfection reagent with the plasmid DNA construct) from 15 minutes (achieved <30% transfection efficiency) to 30 minutes [14-15]. This, resulted in decreased cell culture supernatant collection time (from 6 months to 3

months) (figure 1d). Approximately 700 ml of the cell culture supernatant (CCSN) was purified using Immobilized Affinity Chromatography (IMAC), and elution was made possible through competitive binding between 10x His-tag and Ni^{2+} column. The purified protein fraction was eluted upon the application of increasing imidazole concentration (250 mM) as shown in figure 1(e). The eluted fractions were pulled and resolved on a 10% SDS under denaturing conditions along with different concentration of serially diluted BSA standards to enable quantification by densitometry. The wash and flowthrough fractions were also loaded onto the gel to ensure that the protein effectively bound to the column matrix and if any unbound protein was not lost during the washing step. The gel image clearly showed that the wash and flowthrough fractions did not contain the recombinant fusion protein. The protein band corresponding to the theoretical size of EpCAM (scFv)-SNAP (55kDa) was observed after staining. On the protein lane, higher bands at around 180 kDa, 130kDa, ~100 kDa and slightly visible bands at 72 kDa suggested that the protein purity might be compromised (figure 1f). Due to the presence of these bands, densitometry analysis (not shown) was carried out to estimate the total protein concentration in the sample. It was the first time in our laboratory to achieve a yield of 17 mg/700ml CCSN.

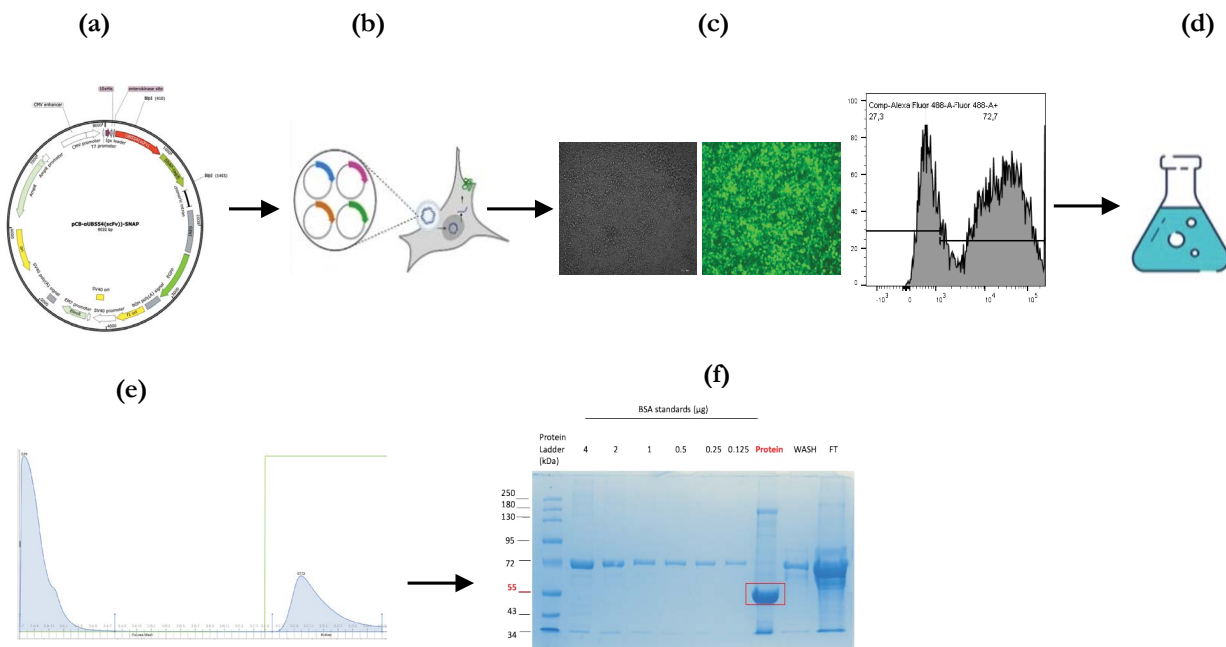


Figure 1: Expression and purification of scFv-SNAP-tag based fusion protein.

(a) Expression plasmid pCB- α EpCAM(scFv)-SNAP was transfected into **(b)** mammalian HEK293T cells. **(c)** Transfected cells were monitored by fluorescent imaging for eGFP expression as an indicator for cells expressing the cloned protein of interest and flow cytometry was used to monitor GFP expression in each transfected cell population. **(d)** Cell culture supernatant was purified using IMAC **(e)**. Bound full length protein was eluted after extensive washing with lower imidazole concentrations. **(f)** The protein of interest containing fractions were concentrated and resolved on a 10 % SDS gel and compared to serially diluted BSA standards to calculate the effective full length protein concentrations.

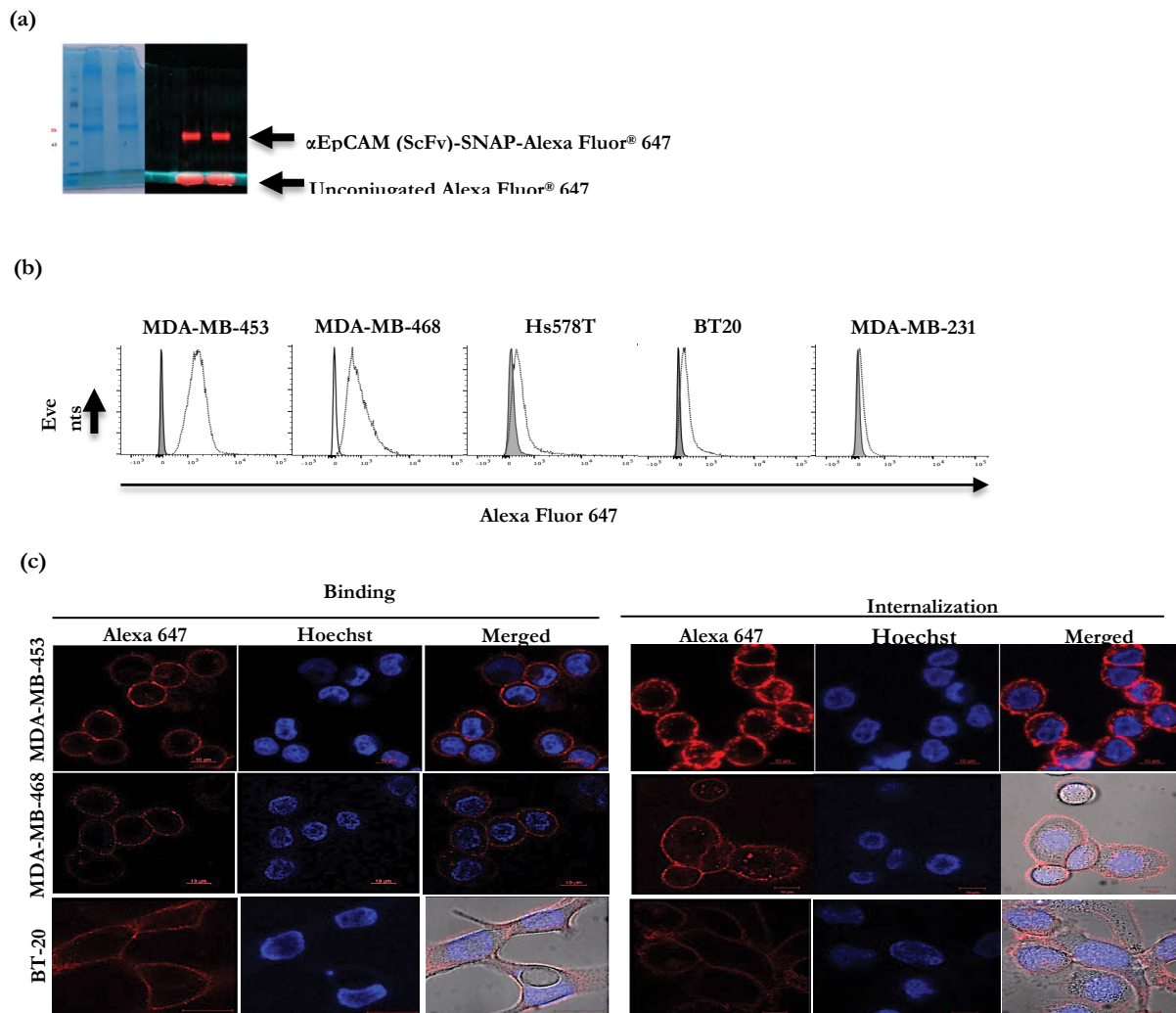


Figure 2: EpCAM expression, binding and internalization in TNBC cell lines.

(a) The fusion protein was conjugated with the SNAP-Surface® Alexa Fluor® 647 in a 1:1 ratio to confirm successful expression of the protein as well as the functionality of the SNAP-tag component. **(b)** Expression level of α EpCAM(scFv)-SNAP-Alexa Fluor® 647 to cell lines was analysed by flow cytometry and, **(c)** Binding and internalization in TNBC cell lines was carried out at 4°C and 37°C for 1 hr and 30 minutes respectively. Images were captured using the Zeiss LSM-880 Airyscan confocal microscope. The red and blue fluorescence represent Alexa Fluor® 647 and Hoechst nuclear stain respectively.

Binding and internalization of the scFv-SNAP-Alexa fluorophores to TNBC and cervical cancer cell lines by flow cytometry and confocal microscopy

After confirming full-length protein by SDS-PAGE, the fusion protein was conjugated with the SNAP-Surface® Alexa Fluor® 647/488 in a 1:1 ratio (figures 2a and 3a). These experiments confirmed (1) the successful expression of the recombinant fusion protein, (2) the functionality of the SNAP-tag component and, (3) initial confirmation that the scFv-SNAP-Alexa fluorophores can be used as imaging agents. This was shown by the fluorescent bands at approximately 55 kDa.

Thereafter, decreased serial dilution of the conjugated fusion protein were incubated with the cells to obtain the optimal antibody binding concentration that will allow a clear distinction between antigen-positive and antigen-negative population for a given cell type using an activated cell sorting BD® LSR II flow cytometer. Figure 2b showed that at the optimal concentration (25 μ g), the expression level of EpCAM in MDA-MB-453 was the highest followed by MDA-MB-468. However, EpCAM expression was minimal in Hs578T and BT20, and very low in MDA-MB-231 cell lines. After demonstrating EpCAM expression, the fusion protein must be effectively internalized into the target cells to exert its potent cytotoxicity activity.

Therefore, the next step was to confirm the binding activity by confocal microscopy. To achieve that, TNBC live cells were incubated with the scFv-Alexa Fluor® 647 at 4°C for 1hr and visualized using the Zeiss LSM-880 Airyscan confocal microscopy. Binding of the fluorescently labelled fusion protein was observed across all cell lines. Upon demonstrating successful binding, the live cells were incubated with the same labelled fusion protein at 37°C for 30 minutes. Internalization was observed in MDA-MB-453 and

minimally in MDA-MB-468 cell lines confirming receptor-mediated endocytosis. However no internalization was observed in BT-20 cell line as expected due to low EpCAM expression (figure 2b)

The cervical cancer cell lines ME-180 and SiHa had the highest and second high EpCAM expression level respectively. Moderate expression was reported on the HeLa cell line and no expression was seen on the negative control cell line HaCaT. The binding of EpCAM targeting SNAP-

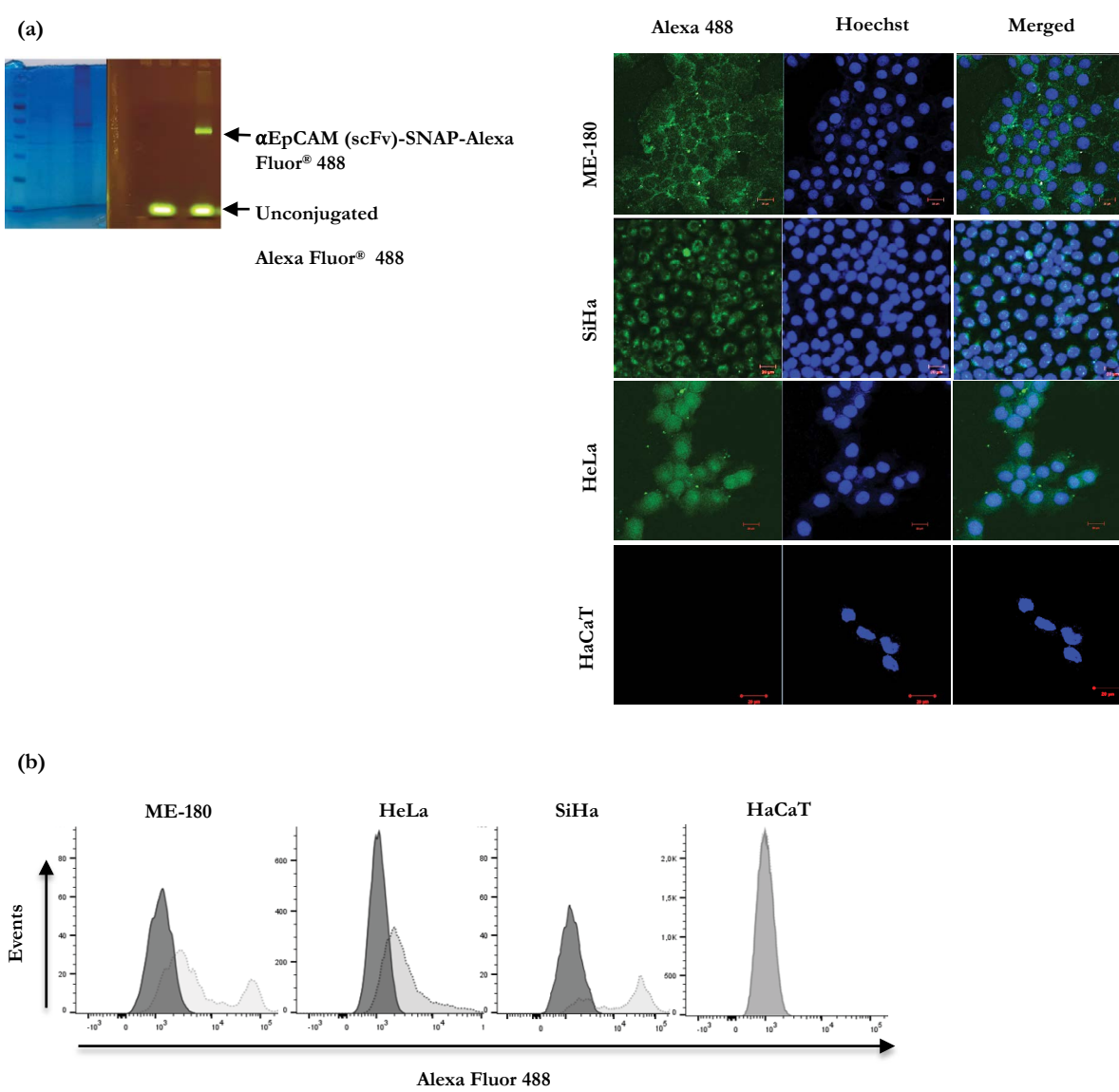


Figure 3: EpCAM expression, binding and internalization in cervical cancer cell lines.

(a) The fusion protein was conjugated with the SNAP-Surface® Alexa Fluor® 488 in a 1:1 ratio to confirm successful expression of the protein as well as the functionality of the SNAP-tag component. **(b)** Expression level of aEpCAM(scFv)-SNAP-Alexa Fluor® 488 to cell lines was analysed by flow cytometry and, **(c)** binding and internalization in cervical cancer cell lines was carried out 37°C for 30 minutes. Images were captured using the Zeiss LSM-880 Airyscan confocal microscope. The green and blue fluorescence represent Alexa Fluor® 488 and Hoechst nuclear stain respectively.

tag fusion protein by treated the cervical cancer cell lines with the fluorophore for 15 minutes at 37°C was assessed by confocal microscopy. The Micrograph images of the cervical cancer cell lines showed internalised green signal across all cell lines when visualized at 40X magnification. The dots of concentrated green signal likely indicated the labelled SNAP-tag based recombinant fusion protein in vesicular transport in the cells, and seen more prominently in ME-180 cell line is the green signal due to the protein label on what appeared to be the cell surface (figure 3c). This data taken together points to the likely mode of internalization of the protein being receptor-mediated endocytosis, with the effect of low environmental temperature on internalization demonstrated in figure 2c with TNBC cell lines. The HaCaT cell line showed no detectable green fluorescence, which in line with the cell surface binding data (figure 3b) indicated low relative expression of EpCAM on this epithelial cell line.

Generation and cytotoxic activity of scFv-SNAP-linker-AURIF (ADC) in cervical and TNBC cell lines

Having confirmed the functionality and integrity of the full-length scFv-SNAP fusion protein, the next goal was to determine whether the fusion protein can be used as a carrier to deliver the anticancer drug into the tumour cells. The purified fusion protein was labelled with 2-fold molar excess BG-linker-AURIF, followed by a post-incubation with the SNAP-Surface® Alexa Fluor® 647, to confirm the full saturation of the fusion protein with BG-linker-AURIF and reconfirm the functionality of the SNAP-tag component. As shown in figure 4a, no fluorescent signal (fluorescent image: scFv-AURIF-A.647) was detected when the gel was visualized using the iBrightFL 1000 imaging system despite the presence of the same labelled protein on the stained SDS-PAGE gel (left image), indicating full saturation of the fusion protein with BG-linker-AURIF. Subsequently, cervical cancer and TNBC cell lines were incubated with decreasing concentration of EpCAM(scFv)-SNAP, BG-linker-AURIF and the ADC, followed by XTT cell viability assay to assess the potential of the immunoconjugate and its controls. The treatment controls (EpCAM(scFv)-SNAP and BG-linker-

AURIF) were included to observe the impact of the ADC and to account for the relative impact of each component of the ADC. The experiments were performed on the cervical cancer cell lines as the effect of these controls in the MDA-MB-468 TNBC cell line have previously been published. [14-15]. The cervical cancer cells treated with BG-linker-AURIF showed killing (IC_{50} values ranging from 359.8nM \pm 3.9 to 414.1nM \pm 3.9), while the cells treated with α EpCAM(scFv)-SNAP depicted no noticeable dose dependent killing. Furthermore, specific and dose-dependent killing was observed for the ADC such that the IC_{50} values observed for the cervical cancer cell lines were 82.97nM \pm 0.07 for SiHa, 82.39nM \pm 5 for ME-180, 121.3nM \pm 6.4 for HeLa (figure 4c) and, 73.31nM \pm 9.5 for MDA-MB-453 TNBC cell line (figure 4b). The generated ADC had no effect on the cervical cancer negative control cell line HaCaT (Figure 4c). Worth noting, is that a dose dependent effect was observed when HaCaT cells were treated with BG-linker-AURIF (741.7nM \pm 62.26), which may be taken as an illustration that the antibody component of the ADC is important for site-directed toxicity such that non-expressing cells may be spared. The recombinant ADC had no effect on the TNBC negative control cell line BT20 (figure 4b) as expected since the fluorescently labelled recombinant fusion protein could not be internalized (figure 2c) due to very low EpCAM expression (figure 2b). Our results showed that a 3 hrs incubation with a 2-fold molar excess of BG-linker-AURIF is more than enough to fully saturate the recombinant fusion protein at room temperature. Table 1 summarizes the IC_{50} values obtained for each cell line.

Discussion

Triple-negative breast cancer or TNBC is a heterogeneous, and aggressive subtype of breast cancer majoritarily affecting women of african ancestry [16-17]. According to the American society of clinical oncology of American pathologists guidelines, TNBCs typically expressed less than 1% oestrogen and progesterone receptors and, between 0-1% HER2 receptor [18]. Cervical cancer is the second most common cancers affecting women in their reproductive age at higher rates than menopausal women in sub-Saharan Africain and, worldwide is expected to rise ~40%

Table 1: Cytotoxicity of the generated ADC against different cervical and TNBC cell lines, represented as half maximal inhibitory concentrations (IC_{50}) values (nM).

Log [BG-linker-AURIF]nM		Log [EpCAM-SNAP-linker-AURIF]nM
ME-180	414.1 \pm 3.9	82.39 \pm 5
SiHa	359.8 \pm 3.9	82.97 \pm 0.07
HeLa	-	121.3 \pm 6.4
HaCaT	741.7 \pm 62.26	Negative control
MDA-MB-453	Previously published	73.31 \pm 9.5
BT20	-	Negative control

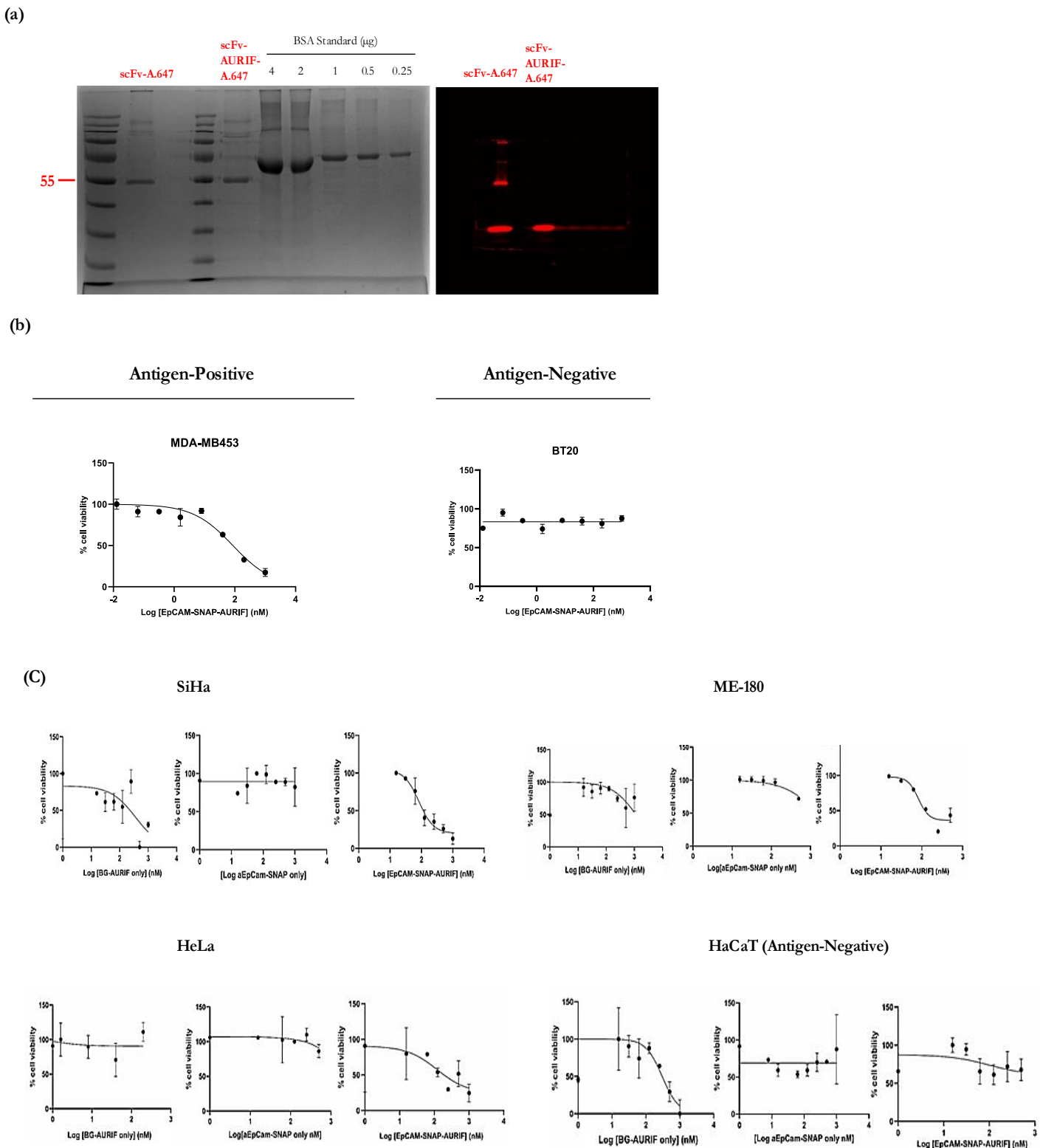


Figure 4: Dose response curve demonstrating the cytotoxic activity of α EpCAM(scFv)-SNAP-linker-AURIF *in vitro*

(a) BG-linker-AURIF was conjugated with α EpCAM (scFv)-SNAP for 3 hours, followed by a post-incubation with the SNAP-Surface® Alexa Fluor® 647, before being loaded on an SDS-PAGE gel, which was visualized using the iBrightFL 1000 imaging system (left panel). Corresponding Aqua stain of SDS-PAGE (right panel). A.647 (SNAP-Surface® Alexa Fluor® 647). XTT cell viability assay was carried out with serial dilution of the BG-linker-AURIF conjugated with scFv-SNAP tag fusion protein in **(b)** TNBC cell lines and **(c)** cervical cancer cell lines. IC_{50} values were calculated using GraphPad Prism 10 software.

Citation: Ursula-Claire Andong-Koung-Edzidzi, Thabo Matshoba, Dirk Lang, Roger Hunter and Stefan Barth. Auristatin F-Delivering SNAP-Tag Based Recombinant Antibody-Drug Conjugate Targeting *EpCAM* Demonstrating Selective In vitro Killing of Cervical and Triple-Negative Breast Cancer Cell Lines. *Journal of Pharmacy and Pharmacology Research*. 10 (2026): 1-14.

in incidence by 2040 [19-20]. While repetitive infection with high risk types of human papillomavirus (HPV) leads to cervical cancer and other types of cancer such as TNBC [21-24], finding a common yet targeted way to combat both cancers, as the two biggest causes of cancer related death in women globally, would be a great public health milestone. Gene expression studies have identified several potentially upregulated pathways which are differentially expressed in the different subtypes of cancer. Therefore, corresponding receptors differentially overexpressed are being considered as high potential diagnostic/therapeutic targets. Such cell receptors have indeed become attractive. Consequently, approximately 60% of the approved FDA protein targeting drugs are directed at cell surface receptors.

EpCAM (epithelial cell-adhesion molecule) is localized on the basolateral membrane of normal epithelial cells or neoplasms derived from epithelia, and also on the surface of human embryonic stem cells. The overexpression of EpCAM is detected in approximately 70-80% of most cancers including TNBC and cervical cancer, and is associated with poor survival rate and higher risk of recurrence. Its abundance on the surface of different cell carcinomas shows that it is one of the most investigated tumour associated antigen. Publication on EpCAM specific ADCs under clinical evaluation is very limited. However, a clinical trial involving CX-2051 which is engineered based on the cymomX Probody masking technology and is armed with a topoisomerase-1 inhibitor payload as well as a conditionally activated interferon alpha 2b has been reported. In the first quarter of 2024, a study enrolling 25 advanced colorectal cancer patients previously treated with irinotecan was initiated. Patients were administered several doses of CX-2051 once every three weeks until April 2025. In May of the same year, they reported that the first two doses (2.4 mg/kg and 4.8 mg/kg) were single patient dose escalation and not anticipated to be effective. For the last three doses (7.2 mg/kg, 8.6 mg/kg, and 10 mg/kg) of the study, 18 out of 23 treated patients were efficacy evaluable. Out of these 18 patients, 5 achieved confirmed partial response evaluation criteria in solid tumors (RECIST), and 3 out of 7 patients treated with the highest dose achieved confirmed partial response. The study also reported a median progression free survival of 5.8 months with no severe side effects even when the doses increased [25].

Numerous approaches have been developed for the conjugation of therapeutic agents to antibodies, but only two are extensively used: the modification of thiol groups in cysteine side chains and the modification of amine group in lysine side chains [26]. In the first method, eight unique cysteine residues are found per antibody, leading to approximately hundred different ADCs [27]. Regarding the second conjugation method, there are approximately forty

unique lysine residues per antibody, therefore approximately 10^6 different ADCs can be produced. Even though these methods are easy to perform, they generate heterogeneous mixtures of ADCs with different pharmacological and safety profiles. Hence, the pharmacokinetics of generated ADCs and unwanted systemic release of the drug can be extremely difficult to estimate. Also, the large size of monoclonal antibodies (150 kDa) and the ADCs derived from them as well as the high cost associated with the production of these complex molecules make them inaccessible to all social classes. Moreover, the off-target effect, limited physiochemical stability and poor tissue penetration affect the therapeutic efficacy of MAbs [28-30]. Our aim was to produce a novel EpCAM (scFv)-specific ADC that is small enough to penetrate cervical cancer and the different TNBC tumour population effectively and, that benefit from efficient conjugation with a defined stoichiometry. The first step was to genetically fused the α EpCAM(scFv) with the SNAP-tag component. Using the SNAP-tag technology allow (1) the defined coupling of BG-modified substrates, (2) the production of fusion protein with no unnatural amino acids, and a size three times (50-55 kDa) less than the full-length monoclonal antibody to facilitate solid tumors penetration time and decrease the retention time in nontarget tumor tissues. The SNAP-tag based recombinant fusion protein can be produced in any expression system such as the mammalian HEK293T cells as previously reported [1-31]. In this regard, enriched α EpCAM(scFv)-SNAP recombinant fusion protein cell culture supernatant was collected and purified with a yield of 17 mg/700 ml which allowed a 1:1 conjugation with the SNAP-Surface®Alexa Fluor® 647 for diagnosis purposes. The expression level of EpCAM was high in MDA-MB-453 followed by a moderate expression in MDA-MB-468, representing basal-like and luminal androgen receptor (LAR) TNBC subtypes respectively, EpCAM expression was minimal in Hs578T and BT20 belonging to the LAR and basal-like TNBC subtypes respectively. However, low EpCAM expression was detected in the mesenchymal (MSL) TNBC Subtype MDA-MB-231. The results generated in MDA-MB-468, MDA-MB-453 and Hs578T cell lines were consistent with previous studies [15-26-32], while other studies reported moderate to weak expression of EpCAM in BT20 cell line [33-34]. Confocal microscopy was used to visualize the binding and internalization of the recombinant fusion protein conjugated with the SNAP-Surface®Alexa Fluor® 647 in TNBC cell lines. The images revealed binding across all selected cell lines, confirming the flow cytometry analysis (figure 2b). The internalization of the conjugate was observed in the basal-like MDA-MB-453 and LAR MDA-MB-468 TNBC subtypes after 30 minutes incubation. Of note, the level of internalization in MDA-MB-468 was minimal compared to MDA-MB-453, probably due to less signal or moderate expression of EpCAM as observed in

figure 2b of this study. Receptor mediated uptake was not observed in the BT20 basal-like subtype due to minimal Expression of EpCAM. Information on EpCAM expression on BT20 is very limited, but this result confirmed a study conducted by Sterzynska et al., 2012 who reported a much lower EpCAM mRNA expression in BT20 cell line, resulting in weak immunofluorescence signal [35]. Currently, TNBC is diagnosed via a combination of three main imaging approaches and immunohistochemistry (IHC). The different imaging tools used include mammogram, ultrasound and magnetic resonance imaging or MRI. The successful detection of TNBC is determined by the presence of high-density tumor with oval or round shape, which cannot be visualized by mammography. Even though ultrasound seems to be more sensitive than mammography, it is difficult to differentiate between benign-like features and benign conditions. MRI has been reported to be highly sensitive than the previous detection tools. However, TNBC can mimic benign condition like cysts or fibroadenomas which can result in misinterpretation [36]. Ideally, IHC is required to detect or confirm the presence of breast cancer as it uses biomarkers staining approaches. To address this aspect of TNBC diagnosis, the fluorescent IHC capacity of the α EpCAM(scFv)-SNAP recombinant fusion protein conjugated with the SNAP-Surface®Alexa Fluor® 647 was demonstrated by its ability to distinguish between human breast tumors and healthy tissues. It was reported specific binding of the fluorescently labelled fusion protein to breast tissues and no significant binding to healthy human tissues, confirming EpCAM as a promising diagnosis marker of TNBC [26].

In addition to diagnosis, the conjugation of the SNAP-tag based recombinant fusion protein with a BG-modified cytotoxic drug allows for the generation of ADCs for the selective killing of target cells. Auristatin F can easily be conjugated to various molecules such as antibodies, is known for being highly hydrophobic, has a low membrane permeability and selectivity for tumor cells, making it a suitable option for targeted cancer therapy [37-40]. As mention earlier, it works by inhibiting the microtubule assembly and tubulin dependent GTP hydrolysis, which results in cell cycle arrest and apoptosis. In the setting of a specific tumor treatment, ideal ADCs should have stable and flexible linkers that will survive during plasma circulation and release the toxic payload at target sites. These ADCs could be engineered in an easy, fast, and efficient manner with high protein yields, thus providing a cheap strategy for the development of novel ADCs. They eliminate cancer cells by binding to the cell surface receptors on the surface of a tumor cell before being internalized into lysosomes where they are degraded by proteases, thereby releasing the active payload into the cytosol to interact with various cellular mechanisms and induce cell death [41]. Various studies have published the

cytotoxic activities of BG-AURIE and BG-AURIF in many carcinomas. The study by Woitok et al., 2016 demonstrated the potency of two EGFR specific scFv-SNAP fusion proteins conjugated to BG-AURIF. The 425(scFv)-SNAP-BG-AURIF and 1711(scFv)-SNAP-BG-AURIF immunoconjugates IC₅₀ values were 4nM for MDA-MB-468 cell line, 8nM and 12 nM for A431 cell line respectively [1]. Another study on the the cytotoxic effect of 1711(scFv)-SNAP-BG-AURIF towards triple-negative breast cancer cell line MDA-MB-468 expressing EGFR reported an IC₅₀ value of 0.516nM [42]. The IC₅₀ value of α CSPG4(scFv)-SNAP-linker-AURIF after incubation with Hs578T triple-negative breast cancer cell line was 173.3nM [43]. Zhang et al. 2022 published a study where they investigated the cytotoxic activity of α EpCAM(scFv) labelled with BG-AURIE using a panel of TNBC cell lines [41]. In the current study, we wanted to understand if replacing BG-AURIE by BG-linker-AURIF will make a significant difference in the IC₅₀ values. We were able to demonstrate this on one of their published TNBC cell line (MDA-MB-453) where EpCAM(scFv)-linker-AURIF had a 4-fold higher activity than BG-AURIE (Table 1). In order to reproduce this relative IC₅₀ value, we further extended our analysis including flow cytometry, confocal microscopy and cell viability assay to EpCAM positive cervical cancer cell lines.

EpCAM(scFv) labelled with the SNAP-Surface®Alexa Fluor® 488 was expressed differently in all EpCAM antigen positive cervical cancer cell lines as shown in figure 3b. After incubation of our antibody with the cell lines for 15 minutes at 37°C, we observed receptor-mediated uptake (figure 3c), similar to figures 2c of this current study and 2a of Zhang et al. publication. The 15-minutes incubation at 37°C, appeared to have allowed for visualization of what is likely the labelled signal concentrated inside large vesicles within the SiHa cell line. Whereas for the HeLa cells the distribution of green signal appeared uniform throughout the cell. To see a clearer internalization with ME-180 cells, a longer incubation time is required (for example 30 minutes as done with the TNBC cell lines) since for the 15 minutes incubation some of the labelled fusion protein appeared to still be on the cell outline. The selective cytotoxic activities of BG-linker-AURIF, scFv-SNAP and the ADC were assessed in three cervical cancer and a keratinocyte cell lines. The scFv-SNAP treatment only did not have any effect on the cell viability as expected. Meaning that the killing of the cells is only possible when BG-linker-AURIF is conjugated to the scFv-SNAP-tag based recombinant fusion protein. The half-maximal inhibitory concentrations for ME-180 and SiHa cell lines were below 100 nM, and slightly higher than 100 nM for HeLa cell line. ME-180 (82.39nM±5), SiHa (82.97nM±0.07), and Hela (121.3nM±6.4) displayed outstanding sensitivity to α EpCAM(scFv)-SNAP-linker-

AURIF compared to IC_{50} values reported by Zhang et al. 2022 (in the range of $135.2\text{nM}\pm 9.6$ to $551\text{nM}\pm 30.76$) using the same antibody but labelled with BG-AURIE. The relative differences between the ME-180, SiHa and HeLa cell lines could be explained by going back to the flow cytometry results (figure 3b), where peaks that shifted on the right of the histogram indicate high signal suggesting high expression of EpCAM as seen in the first two mentioned cell lines. While a peak with a moderate shift indicates low signal probably due to moderate expression of EpCAM such as observed in the Hela cell line, thus affecting internalization. It is important to mention that the IC_{50} values of the BG-linker-AURIF were in the range of $359\text{nM}\pm 3.9$ to $414\text{nM}\pm 9.6$, while those of the same cell lines incubated with the ADC displayed potent IC_{50} values ranging from $82.39\text{nM}\pm 5$ to $121.3\text{nM}\pm 6.4$ implying that AURIF retains its cytotoxicity activity even when it is linked to benzylguanine (BG).

Until as recently as 2017, EpCAM was not considered a suitable immunotherapy target for cervical cancer due to not being seen in significantly high amounts in cervical cancer patient samples by IHC [44]. Hence, the current study sought to break ground with an underexplored immunotherapy target for cervical squamous cell carcinoma, and we observed in this proof-of-concept study that EpCAM is a target that holds promise for low concentration dose-dependent killing of cervical cancer cells through ADCs. The EpCAM targeting

antibody appeared to even confer protection to antigen negative (or low antigen expressing) cells against the cytotoxic payload likely due to high site specificity of the antibody, low expression of the antigen on the cells and the irreversible covalent bond through SNAP-tag that prevents premature release of Auristatin F. Since, Auristatin F has low membrane permeability and thus reduced bystander effects, even when the cells are exposed to this only the HaCaT cell line showed some observable dose-dependent killing with an IC_{50} value much higher than that seen with the ADC compared to the cervical cancer cell lines. In conclusion, this study reports on preliminary analysis of a SNAP-tag based ADC which is a stepping stone for the development of immunodiagnostic and therapeutic tools. Here, we successfully demonstrated that the conjugation of the recombinant fusion protein with different fluorophores and BG-linker-AURIF antimitotic drug was achieved within 1 and 3 hrs for diagnostic and therapeutic purposes respectively. We demonstrated to the best of our knowledge for the first time that EpCAM(scFv)-linker-AURIF was potent against MDA-MB-453 TNBC and all cervical cancer cell lines. Moreover, when comparing the IC_{50} values in the Zhang et al. publication with the current and previously mentioned studies on some of the cell lines, we can confidently conclude that AURIF is more potent than AURIE (Table 2). Future work will be (1) to determine the number of EpCAM receptors per sample and (2) to conduct pre-clinical *in vivo* studies.

Table 2: Comparison of AURIE and AURIF IC_{50} values to demonstrate the potency of Auristatin F.

Cell lines	Authors	ADCs	$IC_{50}(\text{nM})$
MDA-MB-453	Andong et al. 2025	$\alpha\text{EpXAM}(\sigma\chi\Phi\omega)-\Sigma\text{NA}\Pi-\lambda\text{in}\kappa\epsilon\rho-\text{AYPI}\Phi$	73.5 ± 9.5
SiHa			82.97 ± 0.07
HeLa			121.33 ± 6.4
ME-180			83.39 ± 5
MDA-MB-468	Hyuseman et al. 2023	EGFR (1711scFv)-SNAP-linker-AURIF	0.516
Hs578T	Mungra et al. 2023	$\alpha\text{X}\Sigma\text{P}\Gamma\text{4}(\sigma\chi\Phi\omega)-\Sigma\text{NA}\Pi-\lambda\text{in}\kappa\epsilon\rho-\text{AYPI}\Phi$	173.3
MDA-MB-468	Woitok et al. 2016	425(scFv)-SNAP-BG-AURIF	4
		1711(scFv)-SNAP-BG-AURIF	4
A431		425(scFv)-SNAP-BG-AURIF	8
		1711(scFv)-SNAP-BG-AURIF	12
MDA-MB-468	Zhang et al. 2022	EpCAM(scFv)-SNAP-BG-AURIE	551 ± 30.76
MDA-MB-453			-
Hs578T			135.2 ± 9.6
MDA-MB-468			-
MDA-MB-453	EGFR(425scFv)-SNAP-BG-AURIE	740 ± 17.55	
Hs578T			114.7 ± 7.14

Materials & Methods

Cell culture

DMEM supplemented with 10% (v/v) foetal bovine serum (FBS) and 1% (v/v) Pen-Strep (10000U/mL Penicillin, 10000 µg/mL Streptomycin) was used to culture the cervical cancer cell lines HeLa (ATCC CCL-2), SiHa(ATCC HTB-35), ME-180 (ATCC HTB-33), the TNBC cell lines MDA-MB-453 (ATCC cat no. HTB-131), MDA-MB-468 (ATCC cat no. HTB-132), MDA-M-231 (ATCC cat no. HTB-26) and Hs578T (ATCC cat no. HTTB-126) as well as the keratinocyte cell line HaCaT (CVCL_0038). BT-20 (ATCC cat no. HTB-19) was culture in MEM Alpha (1x) supplemented with 10,000 u penicillin, 10 mg streptomycin, 25mg amphotericin B. The cells were all kept in a humidified environment at 37 °C with 5% CO₂.

SNAP-Fusion protein expression and purification

The αEpCAM(ScFv)-SNAP-tag fusion protein was transfected in HEK293T cells cultured in RPMI1640 supplemented with 10% (v/v) FBS and 1% (v/v) Pen-Strep (10000U/mL Penicillin, 10000 µg/mL Streptomycin) using X-tremeGENE™ HP DNA Transfection reagent (Roche, Switzerland). After 96 hours, the cells were washed with 1x PBS, stained with live/dead Alexa Fluor 405 dye, followed by two washes with 1x PBS buffer. The cells were resuspended in FACS buffer prior to determine the transfection efficiency using a BD LSRIFortessa™ II Flow cytometer. The selection of the transfected cells was done with Gibco™ Zeocin™ (100mg/mL) (Thermo Fischer Scientific, USA). Cell culture supernatants were collected and purified using the the Ni2+ Sepharose affinity resin packed in a HisTrap Excel column (GE Healthcare, USA) on an Äkta Avant 25. The eluted fractions were screened for the presence of the fusion protein on a 10% SDS-PAGE analysis gel and stained with AcquaStain Protein Gel Stain (Bulldog-Bio, USA).

Binding activity by flow cytometry

The purified protein containing the SNAP-tag was first labelled with the SNAP-Surface® Alexa Fluor® 647/488 in a 1:1 molar ratio to confirm the functionality of the SNAP-tag component and expression of the protein of interest. Thereafter, 5x10⁵ cells were washed with 1x PBS and incubated with both fluorophores separately for 1 hour in 50 ml PBS on ice. The binding of the labelled fusion protein to cervical and TNBC cells lines as well as the keratinocyte cell line was monitored by flow cytometry on a BD LSRIFortessa™ II flow cytometer (BD Biosciences, USA), and analysis was done on a Flow Jo v10.9.0 software.

Binding and internalization by confocal microscopy

Cervical cancer cell lines HeLa, SiHa, ME-180 and HaCat cells were seeded overnight on 22mm x22mm coverslips placed inside 6 well plates such that 1x10⁴ cells are seeded

on the slip. A volume of 200 µl of the SNAP-Surface® Alexa Alexa Fluor® 488 conjugated protein was added on to the cells, along with Hoechst fluorescent nuclear stain (1:5000 in non-supplemented DMEM) and incubated at 37 °C for 30 minutes. Fixing with 4% Paraformaldehyde was done for 20 minutes following by a 1x PBS wash step. The paraformaldehyde was washed off with 1x PBS before mounting the coverslip on a slide and left in the dark, overnight. TNBC cell lines MDA-MD-468, MDA-MD-453 and BT20 were seeded in a live viewing dish (four quadrants) to a density of 5x10⁴ cells and incubated at 37°C for 24 hours. To validate the binding and internalization, cells were incubated with SNAP-Surface® Alexa Fluor® 647 labelled SNAP-tag fusion protein at 4°C (binding) and 37°C (internalization) for 10 minutes and 30 minutes respectively. After two washing steps with 1 x PBS, the cells were incubated with Hoechst for 10 minutes before washing with PBS to remove excess stain. They were then incubated with their respective media before images were captured using the LSM 880 Airyscan confocal microscope (Zeiss).

Generation of scFv-BG-linker-AURIF antibody drug conjugate (ADC)

Briefly, 2-fold molar excess of BG-linker-AURIF synthesized by the chemistry department of the University of Cape Town [42] was incubated with 1-fold of the αEpCAM(scFv)-SNAP-tag recombinant fusion protein for 3 hours at 37°C. To confirm the successful conjugation, 15µL of the ostensibly conjugated protein was aliquoted and incubated with the SNAP-Surface® Alexa Fluor® 647/488 and subsequently loaded on a 10% SDS-PAGE gel. Thereafter, the unconjugated BG-linker-AURIF was removed using a 10K amicon column by centrifugation. When the saturation of the fusion protein with BG-linker-AURIF was achieved, 5x10³ cells were seeded in a 96 well plate and allowed to adhere overnight before incubation with serial dilution of the antibody drug conjugate (ADC) in triplicate. At 72 hours after the initial treatments, XTT reagent (Roche, Switzerland) was added to the wells and the cells were incubated for 4 hours at 37°C. The reduced XTT to an orange formazan dye was measured at a 450 nM absorbance wavelength and 650 nM reference wavelength on a spectrophotometer. The readings were normalized between the two controls (positive: Zeocin or DMSO and negative control: media without cells) using GraphPad Prism v.10 software to obtain the IC₅₀ value.

Statistical analysis

The quantitative experiments were carried out in triplicate with at least 2 repeats. The flow cytometry results were analysed in Flow Jo v10.9.0. The XTT results were organised on MS Excel and the determination of the half maximal inhibitory concentration (IC₅₀) was done on GraphPad Prism (GraphPad Software, USA). The IC₅₀ are presented as IC₅₀ ± SD.

Author contributions

Conceptualization: UC Andong-Koung-Edzidzi and S Barth; Writing original draft: UC Andong-Koung-Edzidzi; Methodology: UC Andong-Koung-Edzidzi and T Matshoba; Editing: UC Andong-Koung-Edzidzi and T Matshoba; References: UC Andong-Koung-Edzidzi; Critical analysis: S Barth, R Hunter, and D Lang; Final review: S Barth. All authors have read and agreed to the published version of the manuscript.

Acknowledgements

We would like to thank the University of Cape Town (UCT), National Research Foundation (NRF) and the Harry Crossley Foundation Postgraduate Scholarship for funding this project. My amazing supervisor Prof. Dr. Stefan Barth, for his expertise, excellent supervision, constant advice, kindness, understanding, love, and support. Profs. Dirk Lang, Edward Sturrock, Roger Hunter, and Dr. Tim Reid thank you for your assistance in terms of infrastructure and technical support.

Funding

This was partially supported by The South African Research Chairs Initiative of the Department of Science and Technology administered through the National Research Foundation of South Africa (Grant Number 47904) as well as the University of Cape Town Vision 2030 Grand Challenges Initiative.

Ethics approval

Approval for the use of the cell lines was obtained from the Human research ethics committee, University of Cape Town, South Africa (Reference number: C024/2025 and C013/2024)

Conflicts of interest

The authors have no conflicts of interest.

References

1. Woitok M, Klose D, Di Flore S, et al. Comparison of a mouse and a novel human scFv-SNAP-auristatin F drug conjugate with potent activity against EGFR-overexpressing human solid tumor cells. *OncoTargets and Therapy* 10 (2017): 3313-3327.
2. Woitok M, Klose D, Niesen J, et al. The efficient elimination of solid tumor cells by EGFR-specific and HER2-specific scFv-SNAP fusion proteins conjugated to benzylguanine-modified auristatin F. *Cancer Letters* 381 (2016): 323-330.
3. Ponziani S, Di Vittorion G, Pitari G, et al. Antibody-drug conjugates: The new frontier of chemotherapy. *International Journal of Molecular Sciences* 21 (2020): 5510.
4. Kim EG, Kim KM, et al. Strategies and advancement in antibody-drug conjugate optimization for targeted cancer therapeutics. *Biomolecules and Therapeutics (Seoul)* 23 (2015): 493-509.
5. Chen H, Lin Z, Arnst KE, et al. Tubulin inhibitor-based antibody-drug conjugates for cancer therapy. *Molecules* 22 (2017): 1281.
6. Staudacher AH, Brown MP, et al. Antibody-drug conjugates and bystander killing: Is antigen-dependent internalisation required? *British Journal of Cancer* 117 (2017): 1736-1742.
7. Shastry M, Gupta A, Chandarlapaty S, et al. Rise of antibody-drug conjugates: The present and future. *ASCO Educational Book* 43 (2023): e390094.
8. Imrich S, Hachmeister M, Gires O, et al. EpCAM and its potential role in tumor-initiating cells. *Cell Adhesion and Migration* 6 (2012): 30-38.
9. Armstrong A, Eck SL, et al. EpCAM: A new therapeutic target for an old cancer antigen. *Cancer Biology & Therapy* 2 (2003): 320-326.
10. Huang L, Yang Y, Yang F, et al. Functions of EpCAM in physiological processes and diseases. *International Journal of Molecular Medicine* 42 (2018): 1771-1785.
11. Schmidt M, Rüttinger D, Sebastian M, et al. Phase IB study of the EpCAM antibody adecatumumab combined with docetaxel in patients with EpCAM-positive relapsed or refractory advanced-stage breast cancer. *Annals of Oncology* 23 (2012): 2306-2313.
12. Salnikov AV, Groth A, Apel A, et al. Targeting of cancer stem cell marker EpCAM by bispecific antibody EpCAMxCD3 inhibits pancreatic carcinoma. *Journal of Cellular and Molecular Medicine* 13 (2009): 4023-4033.
13. Dogbey DM, Andong-Koung-Edzidzi UC, Molope GA, et al. EpCAM-targeting cancer immunotherapies: Evidence from clinical studies and the way forward. *Tumor Discovery* 4 (2024): 1-13.
14. Mungra N, et al. Development of SNAP-tag based fusion proteins as novel auristatin F-containing immunoconjugates and photoimmunotheranostics in the detection and treatment of triple-negative breast cancer. Doctoral dissertation, University of Cape Town (2021).
15. Madheswaran S, et al. Evaluation of tumour-associated antigens to optically label cutaneous basal cell carcinoma for surgical excision. Doctoral dissertation, University of Cape Town (2022).

16. Honorio M, Guerra Pereira N, et al. Decreased survival in African patients with triple negative breast cancer. *Journal of Palliative Care & Medicine* 6 (2016): 270.
17. Wu Q, Siddharth S, Sharma D, et al. Triple-negative breast cancer: A mountain yet to be scaled despite the triumphs. *Cancers (Basel)* 13 (2021): 3697.
18. Almansour NM, et al. Triple-negative breast cancer: A brief review about epidemiology, risk factors, signaling pathways, treatment and role of artificial intelligence. *Frontiers in Molecular Biosciences* 9 (2022): 836417.
19. Phimsen W, Kopitak N, Boontawon T, et al. Optimizing the production of recombinant human papilloma virus type 52 major capsid protein L1 in *Hansenula polymorpha*. *Scientific Reports* 14 (2024): 28555.
20. Biziayehu HM, Dadi FA, Hassen TA, et al. Global burden of 34 cancers among women in 2020 and projections to 2040. *International Journal of Cancer* 154 (2024): 1377–1393.
21. Piana AF, Sotgiu G, Muroni MR, et al. HPV infection and triple-negative breast cancers: An Italian case-control study. *Virology Journal* 11 (2014): 190.
22. De Carolis S, Storci G, Ceccarelli C, et al. HPV DNA associates with breast cancer malignancy and is transferred to stromal cells by extracellular vesicles. *Frontiers in Oncology* 9 (2019): 860.
23. Sosse SA, Ennaji Y, Tiabi I, et al. The involvement of human papillomavirus in breast cancer and prognostic biomarkers in triple-negative breast cancer. *Oncogenic Viruses* 1 (2023): 335–357.
24. Parviainen E, Nurmenniemi S, Ravaioli S, et al. Human papillomavirus E6 alters Toll-like receptor 9 transcripts and chemotherapy responses in breast cancer cells. *Molecular Biology Reports* 52 (2024): 43.
25. CytomX Therapeutics, et al. CytomX announces positive interim data from phase 1 dose escalation study of EpCAM antibody-drug conjugate CX-2051. Press Release (2025).
26. Amoury M, Bauerschlag D, Zeppernick F, et al. Photoimmunotherapeutic agents for triple-negative breast cancer diagnosis and therapy. *Oncotarget* 7 (2016): 54925–54936.
27. Diamantis N, Banerji U, et al. Antibody-drug conjugates—An emerging class of cancer treatment. *British Journal of Cancer* 114 (2016): 362–367.
28. Castelli MS, McGonigle P, Hornby PJ, et al. Pharmacology and therapeutic applications of monoclonal antibodies. *Pharmacology Research & Perspectives* 7 (2019): e00535.
29. Chames P, Van Regenmortel MV, Weiss E, et al. Therapeutic antibodies: Successes, limitations and hopes for the future. *British Journal of Pharmacology* 157 (2009): 220–233.
30. Weiner GJ, et al. Building better monoclonal antibody-based therapeutics. *Nature Reviews Cancer* 15 (2015): 361–370.
31. Agarwal P, Bertozzi CR, et al. Site-specific antibody-drug conjugates. *Bioconjugate Chemistry* 26 (2015): 176–192.
32. Amoury M, et al. EpCAM and CSPG4 scFv-based fusion proteins for the treatment of triple-negative breast cancer. Doctoral dissertation, RWTH Aachen University (2017).
33. Mostert B, Kraan J, Bolt-de Vries J, et al. Detection of circulating tumor cells in breast cancer. *Breast Cancer Research and Treatment* 127 (2011): 33–41.
34. Hughes AD, Marshall JR, Keller E, et al. Differential drug responses of circulating tumor cells. *Cancer Letters* 352 (2014): 28–35.
35. Sterzynska K, Kempisty B, Zawierucha P, et al. Specificity and selectivity of anti-EpCAM antibodies in breast cancer cell lines. *Folia Histochemica et Cytobiologica* 50 (2012): 534–541.
36. Ye Z, Ma M, Chen Y, et al. Early diagnosis of triple-negative breast cancer based on dual microRNA detection. *Analytical Chemistry* 96 (2024): 17984–17992.
37. Smith LM, Nesterova A, Alley SC, et al. Potent cytotoxicity of an auristatin-containing antibody-drug conjugate. *Molecular Cancer Therapeutics* 5 (2006): 474–482.
38. Bouchard H, Viskov C, Garcia-Echeverria C, et al. Antibody-drug conjugates: A new wave of cancer drugs. *Bioorganic & Medicinal Chemistry Letters* 24 (2014): 5357–5363.
39. Li H, Yu C, Jiang J, et al. Anti-HER2 antibody conjugated with monomethyl auristatin E. *Cancer Biology & Therapy* 17 (2016): 346–354.
40. Parslow AC, Parakh S, Lee FT, et al. Antibody-drug conjugates for cancer therapy. *Biomedicines* 4 (2016): 14.
41. Zhang C, Sheng W, Al-Rawe M, et al. EpCAM- and EGFR-specific antibody-drug conjugates for triple-negative breast cancer. *International Journal of Molecular Sciences* 23 (2022): 6122.
42. Huysamen AM, Fadeyi OE, Mayuni G, et al. Click chemistry-generated auristatin F-linker-benzylguanine for SNAP-tag-based ADCs. *ACS Omega* 8 (2023): 4026–4037.

43. Mungra N, Biteghe FA, Malindi Z, et al. CSPG4 as a target for triple-negative breast cancer treatment. *Journal of Cancer Research and Clinical Oncology* 149 (2023): 12203–12225.

44. Chantima W, Thepthai C, Cheunsuchon P, et al. EpCAM expression in squamous cell carcinoma of the uterine cervix. *BMC Cancer* 17 (2017): 811.



This article is an open access article distributed under the terms and conditions of the
[Creative Commons Attribution \(CC-BY\) license 4.0](#)